Linear polyatomic molecules with Π ground state: Sensitivity to variation of the fundamental constants

M. G. Kozlov
Petersburg Nuclear Physics Institute, Gatchina 188300, Russia
and St. Petersburg Electrotechnical University "LETI," Russia
(Received 3 February 2013; published 7 March 2013)

In polyatomic molecules with a Π electronic ground state, the rovibrational spectrum can be strongly modified by the Renner-Teller effect (the coupling between bending vibrational mode and electrons in the degenerate Π state). The linear form of the C_3H molecule has particularly strong Renner-Teller interactions and a very-low-lying vibronic $\Sigma^+_{1/2}$ level, which corresponds to the excited bending vibrational mode. This leads to the increased sensitivities of the microwave and submillimeter transition frequencies to the possible variation of the fine structure constant α and electron-to-proton mass ratio μ.

DOI: 10.1103/PhysRevA.87.032104 PACS number(s): 06.20.Jr, 06.30.Ft, 33.20.Bx

I. INTRODUCTION

At present it is generally recognized that microwave and submillimeter molecular spectra from the interstellar medium provide us with a very sensitive tool to study possible variation of the fundamental constants $\alpha = e^2/\hbar c$ and $\mu = m_e/m_p$ on a large spacetime scale. It was shown that certain types of transitions are particularly sensitive to such variations. The mixed tunneling-rotational transitions in molecules such as H_3O^+, H_2O_2, CH_3OH, and CH_3NH_2 can be very sensitive to μ variation [1–6]. Recently, the submillimeter spectra of methanol have been used to place very stringent limits on μ variation on the cosmological timescale [5,7]. On the other hand, the Λ-doublet transitions in diatomic radicals such as OH and CH are very sensitive to variations in both constants [8–10]. The 18 cm OH line was observed at high redshifts, which constrained the time variation of both constants [11]. In that work the 21 cm hyperfine hydrogen line was used as a reference. This constraint can be further improved if more than one Λ-doublet transition in OH or CH is detected.

A rather general way to look for the enhanced sensitivity to variation in the fundamental constants is to search for the accidental degeneracy of levels of different nature. This approach works for very different systems from nuclei, to atoms, and molecules (see, for example, the reviews [12] and [13]).

In this paper we want to draw attention to the microwave and submillimeter spectra of the linear polyatomic radicals with nonzero electronic angular momentum. First, these molecules have K doublets, which are analogous to the Λ doublets in diatomics. Second, the Renner-Teller interaction can lead to the anomalously-low-lying vibronic levels and cause enhanced sensitivities of the mixed rovibronic transitions. Finally, there are many linear polyatomic molecules which are detected in the interstellar medium. In this context one of the most interesting species is the linear C_3H molecule, where the excited vibronic $\Sigma^+_{1/2}$ level lies less than 30 cm^{-1} above the ground level $\Pi_{1/2}$ and where several mixed transitions were recently measured in a molecular beam experiment [14]. Because of that we focus on this molecule here, leaving other similar molecules for a separate discussion.

The interstellar carbon-chain radicals of hydrocarbon series C_nH ($n = 2$–6) exist in linear and cyclic isomeric forms. Both forms are observed in the millimeter-wave range toward dark and translucent molecular clouds and circumstellar envelopes of carbon-rich stars [15–27]. A typical abundance of the linear radical l-C_3H—the simplest odd-carbon chain radical under consideration in the present study—is $\sim 10^{-9}$ relative to hydrogen. The cyclic-to-linear abundance ratio [c-C_3H]/[l-C_3H] ∼5−10 in dark clouds [23,25] but decreases to ∼3 in translucent clouds [23] and becomes less than unity around carbon stars [27]. The cyclic and linear isomers of C_3H have also been detected in a star-forming region [28] and in two extragalactic sources: the star-burst galaxy NGC 253 [29] and the spiral galaxy located in front of the quasar PKS 1830–211 at the redshift $z = 0.89$ [30]. Thus, l-C_3H lines have been detected in regions with kinetic temperature ranging from $T_{\rm kin} \sim 10$ K (dark clouds) to several hundred Kelvin (circumstellar envelopes, star-forming regions). The observed line intensities are less than or about 0.1 K.

The lines observed from the interstellar medium (ISM) are Doppler broadened, so the linewidth $\Gamma \approx \Gamma_D = \omega \frac{\Delta V}{c}$, where ΔV is the velocity distribution for the ISM and c is speed of light. This means that $\frac{\Gamma}{\omega} \approx \frac{\Delta V}{c}$ characterizes ISM and to a first approximation is independent of the frequency ω of the transition. Because of that, for the astrophysical search of the possible variation of the fundamental constants, it is crucial to find transitions with high dimensionless sensitivity coefficients defined as

$$\frac{\delta\omega}{\omega} = Q_\alpha \frac{\delta\alpha}{\alpha} + Q_\mu \frac{\delta\mu}{\mu}. \tag{1}$$

In the optical waveband these sensitivity coefficients are typically of the order of 10^{-2}. In the microwave waveband they are typically of the order of unity but can be much bigger. Below we will calculate Q factors for some microwave and submillimeter transitions of the l-C_3H molecule and show that they can reach the order 10^3. As usual such enhanced sensitivities take place for the low-frequency transitions between quasidegenerate levels of different nature.

II. RENNER-TELLER EFFECT

In this section we briefly recall the theory of the Renner-Teller effect in polyatomic linear molecules [31,32]. The total molecular angular momentum $\boldsymbol{J}$ consists of several

contributions. We have the overall rotation $\boldsymbol{R}$ of the nuclei. Then we have the vibrational angular momentum $\boldsymbol{G}$ associated with the twofold degenerate bending vibration mode(s) and the electronic angular momentum $\boldsymbol{L}$. Momentum $\boldsymbol{R}$ is perpendicular to the molecular axis ζ; two others have ζ projections l and Λ. We define momentum $\boldsymbol{N} = \boldsymbol{R} + \boldsymbol{G} + \boldsymbol{L}$ and its projection $\langle N_\zeta \rangle = K = l + \Lambda$. Finally, we add electronic spin: $\boldsymbol{J} = \boldsymbol{N} + \boldsymbol{S}$, $\langle J_\zeta \rangle = \Omega$.

Suppose we have a Π electronic state $|\Lambda = \pm 1\rangle$ and a $v = 1$ vibrational state of a bending mode $|l = \pm 1\rangle$. All together there are four states $|\Lambda = \pm 1\rangle|l = \pm 1\rangle$. We can rewrite them as one doublet Δ state $|K = \pm 2\rangle$ and states Σ^+ and Σ^-. In the adiabatic approximation all four states are degenerate. Renner [31] showed that the states with the same quantum number $K = l + \Lambda$ strongly interact, so Σ^+ and Σ^- states repel each other, while the Δ doublet in the first approximation remains unperturbed. We are particularly interested in the case when one of the Σ levels is pushed close to the ground state $v = 0$. This is what takes place in l-C_3H molecule [14,19,33].

Consider a linear polyatomic molecule with an unpaired electron in the π_ξ state in the molecular frame ξ, η, ζ. Obviously, the bending energy is different for bendings in the $\xi\zeta$ than in $\eta\zeta$ planes: $V_\pm = \frac{1}{2}k_\pm \chi^2$ (here χ is the supplement to the bond angle). That means that the electronic energy depends on the angle ϕ between the electron and nuclear planes:

$$H' = V' \cos 2\phi, \tag{2}$$

where $2V' = V_+ - V_- = k'\chi^2$. There is no reason for V' to be small, so $k' \sim k_\pm \sim 1$ a.u. and to a first approximation k' does not depend on α and μ.

As long as interaction (2) depends on the relative angle between electron and vibrational rotation it changes angular quantum numbers as follows: $\Delta\Lambda = -\Delta l = \pm 2$ and $\Delta K = 0$. This is exactly what is necessary to produce splitting between Σ^+ and Σ^- states with $v = 1$ as discussed above.

Interaction (2) also mixes different vibrational levels with $\Delta v = \pm 2, \pm 4, \ldots$. Thus, we have, for example, the nonzero matrix element (ME) $\langle 0,0,1,1|H'|2,2,-1,1\rangle$ between states $|v,l,\Lambda,K\rangle$. Such mixings reduce the effective value of the quantum number Λ and, therefore, reduce the spin-orbit splitting between the $\Pi_{1/2}$ and $\Pi_{3/2}$ states [34],

$$H_{\rm so} \equiv A_{\rm eff}\Lambda\Sigma, \quad A_{\rm eff} = A\Lambda_{\rm eff}/\Lambda. \tag{3}$$

Let us define the model more accurately. Following Ref. [34] we write Hamiltonian as

$$H = H_e + T_v + AL_\zeta S_\zeta. \tag{4}$$

Here "electronic" part H_e includes all degrees of freedom except for the bending vibrational mode and spin. For l-C_3H there are two bending modes, but for simplicity we include the second bending mode in H_e, too. Electronic MEs in the $|\Lambda\rangle$ basis have the form

$$\langle \pm 1|H_e|\pm 1\rangle = \frac{V_+ + V_-}{2} = \frac{k}{2}\chi^2, \tag{5a}$$

$$\langle \pm 1|H_e|\mp 1\rangle = \frac{k'}{2}\chi^2 \exp(\mp 2i\phi). \tag{5b}$$

Here χ and ϕ are vibrational coordinates for the bending mode. Kinetic energy in these coordinates has the form

$$T_v = -\frac{1}{2MR^2}\left(\frac{\partial^2}{\partial\chi^2} + \frac{1}{\chi}\frac{\partial}{\partial\chi} + \frac{1}{\chi^2}\frac{\partial^2}{\partial\phi^2}\right). \tag{6}$$

We can use the basis set of two-dimensional (2D) harmonic functions in polar coordinates $\rho = \chi R$ and ϕ for the mass M and force constant k:

$$\psi_{v,l}(\rho,\phi) = R_{v,l}(\rho)\frac{1}{\sqrt{2\pi}}\exp(il\phi). \tag{7}$$

It is important that radial functions are orthogonal only for the same l:

$$\langle R_{v',l}|R_{v,l}\rangle = \delta_{v',v}. \tag{8}$$

This allows for the nonzero MEs between states with different quantum number l. Averaging operator (4) over vibrational functions we get

$$\langle v',l'|H_e + T_v|v,l\rangle = [\omega_v(v+1) + A\Lambda S_\zeta]\delta_{v',v}\delta_{l',l} + \tfrac{1}{2}\langle R_{v'l'}|k'\chi^2|R_{vl}\rangle \exp(\mp 2i\phi)\delta_{l',l\pm 2}. \tag{9}$$

The exponent here ensures the selection rule $\Lambda' = \Lambda \mp 2$ for the quantum number Λ when we calculate MEs for the rotating molecule.

We solved the eigenvalue problem for Hamiltonian (4) using the basis set of the 2D harmonic oscillator. Matrix elements were formed according to Eq. (9). As discussed above we neglected one of the bending modes leaving only the one that produces $K = 0$ level close to the ground-state doublet $K = 1, \Omega = 1/2,3/2$. Our model Hamiltonian has only three parameters; namely ω_v, A, and the dimensionless Renner-Teller parameter $\mathcal{E}$: $k' = \mathcal{E}k$. In Ref. [34] the following values were obtained:

$$\omega_v = 589\ {\rm cm}^{-1}, \quad A = 29\ {\rm cm}^{-1}, \quad \mathcal{E} = 0.883. \tag{10}$$

We fixed the values for ω_v and A and varied the Renner-Teller parameter $\mathcal{E}$ to fit five lowest levels for the given bending mode: $\Pi_{1/2}$, $\Pi_{3/2}$, $\Sigma_{1/2}$, $\Delta_{3/2}$, and $\Delta_{5/2}$. The optimal value appeared to be $\mathcal{E} = 0.788$. The difference with Eq. (10) is probably due to the neglect of the anharmonic corrections and second bending mode.

Our results are presented in Table I. The first two columns give nominal vibrational quantum number v and its actual average value. We see that Renner-Teller term in Eq. (9) strongly mixes vibrational states. This mixing also affects $\langle\Lambda\rangle$ and decreases spin-orbital splittings as explained by Eq. (3).

TABLE I. Low-lying energy levels for the bending mode $\omega_v = 589\ {\rm cm}^{-1}$ and their sensitivities q_α and q_μ to the variation of α and μ, respectively. All values are in ${\rm cm}^{-1}$.

$v_{\rm nom}$	$\langle v\rangle$	K	Ω	$\langle\Lambda\rangle$	E	Δ	[34]	q_μ	q_α
0	1.22	1	0.5	0.50	367.9	0.0	0.0	187.8	−14.6
0	1.35	1	1.5	0.46	381.9	13.9	14.0	187.8	13.3
1	2.32	0	0.5	−0.01	394.2	26.3	27.0	197.3	−0.4
1	3.57	2	1.5	0.21	597.7	229.7	226.0	300.3	−6.1
1	3.65	2	2.5	0.19	603.5	235.5	232.0	300.3	5.5

TABLE II. Q factors for the transitions between states from Table I and for parameters $A_{\rm eff}$ and $\Delta E_{\Sigma\Pi}$ defined by Eqs. (3) and (11), respectively. Frequencies are in cm^{-1}.

				Fit to Ref. [34]			Fit to Ref. [14]		
K	Ω	K'	Ω'	ω	Q_μ	Q_α	ω	Q_μ	Q_α
1	0.5	1	1.5	13.9	0.00	2.00	14.4	0.00	2.00
1	1.5	0	0.5	12.4	0.78	−1.11	13.3	0.77	−1.07
0	0.5	2	1.5	203.5	0.51	−0.03	204.4	0.51	−0.03
2	1.5	2	2.5	5.8	0.00	2.00	6.0	0.00	2.00
	$A_{\rm eff}$			13.9	0.00	2.00	14.4	0.00	2.00
	$\Delta E_{\Sigma\Pi}$			19.4	0.50	0.00	20.5	0.50	0.00

The last two columns in Table I give the sensitivity coefficients q_α and q_μ in cm^{-1}:

$$\delta E = q_\alpha \frac{\delta\alpha}{\alpha} + q_\mu \frac{\delta\mu}{\mu}.$$

To get them we assumed that parameters (10) scale in a following way: $\omega_v \sim \mu^{1/2}$, $A \sim \alpha^2$, and $\mathcal{E}$ does not depend on α and μ. The dimensionless sensitivity coefficients (1) for the transitions $\omega_{i,k} = E_k - E_i$ can be found as

$$Q_{i,k} = (q_k - q_i)/\omega_{i,k}.$$

In Table II these coefficients are calculated for the same set of parameters as in Table I and for the slightly different parameters which better fit experimental frequencies from Ref. [14]. We see that Q factors are practically the same for both sets.

For the two fine-structure transitions $\Pi_{1/2} \longrightarrow \Pi_{3/2}$ and $\Delta_{3/2} \longrightarrow \Delta_{5/2}$, we get sensitivities $Q_\mu = 0$ and $Q_\alpha = 2$. This may seem strange because the fine structure is significantly reduced by Renner-Teller mixing: the fine-structure parameter is 29 cm^{-1} and the splitting between $\Pi_{1/2}$ and $\Pi_{3/2}$ is only 13.9 cm^{-1}. According to Eq. (3) the mixing reduces the splitting. However, this effect depends on the dimensionless Renner-Teller parameter $\mathcal{E}$ and does not depend on μ and α. Consequently, the effective parameter $A_{\rm eff}$ depends on the fundamental constants in the same way as initial parameter A.

For the high-frequency transition $\Sigma_{1/2} \longrightarrow \Delta_{3/2}$, where spin-orbital energy can be neglected, we get $Q_\mu = 0.5$ and $Q_\alpha = 0$. These results are expected, because our model has only two-dimensional parameters: vibrational frequency, which is proportional to $\mu^{1/2}$ and the fine-structure parameter A, which scales as α^2. Even though our vibrational spectrum is far from that of a simple harmonic oscillator, the nondiagonal MEs (9) of the Hamiltonian (4) still scale as $\mu^{1/2}$. Therefore, if we neglect spin-orbital splittings, we get $Q_\mu = 1/2$ for all transitions. The only transition in Table II where spin-orbit energy and vibrational energy are close to each other is the $\Pi_{3/2} \longrightarrow \Sigma_{1/2}$ transition. The resultant frequency is roughly half of the vibrational energy difference between Π and Σ states. This leads to $Q_\mu \approx 1$ and $Q_\alpha \approx -1$.

The following analysis in Sec. III will be based on the effective Hamiltonian for the rotating molecule. The latter includes only two parameters from this section: the effective fine-structure parameter $A_{\rm eff}$ and the energy difference between Σ and Π states,

$$\Delta E_{\Sigma\Pi} = E(\Sigma^+) - \frac{E(\Pi_{1/2}) + E(\Pi_{3/2})}{2}. \qquad (11)$$

Numerical values for these parameter will be obtained from the fit to experimental transition frequencies. Here we only need to determine the dependence of these parameters on fundamental constants. Table II shows that $A_{\rm eff} \sim \alpha^2$ and $\Delta E_{\Sigma\Pi} \sim \mu^{1/2}$. Once again, this is because the Renner-Teller mixing depends on the dimensionless parameter $\mathcal{E}$ and *does not* depend on α and μ.

III. EFFECTIVE HAMILTONIAN FOR ROTATING MOLECULE

In this section we mostly follow Ref. [14]. However, we prefer to use the basis set for Hund's case "a" as we did before [10,35]. We define the effective Hamiltonian for the subspace of the three lowest vibronic states $\Pi_{1/2}$, $\Pi_{3/2}$, and $\Sigma^+_{1/2}$. We neglect some minor centrifugal corrections included in Ref. [14].

The basis rovibronic states for Hund's case "a" have the form

$$|v,l,\Lambda,(K),S,\Sigma,J,\Omega,M\rangle = |v,l\rangle|\Lambda\rangle|S,\Sigma\rangle|J,\Omega,M\rangle.$$

Here the quantum number K does not appear explicitly, being defined as $K = l + \Lambda$. From these basic states we form parity states as described in Ref. [36]:

$$\begin{aligned}|\Pi_{1/2}\rangle &= \left|0,0,1,(1),\frac{1}{2},-\frac{1}{2},J,\frac{1}{2},M,p\right\rangle \\ &= \frac{1}{\sqrt{2}}|0,0\rangle\left(|1\rangle\left|\frac{1}{2},-\frac{1}{2}\right\rangle\left|J,\frac{1}{2},M\right\rangle\right. \\ &\quad \left. + \chi_p|-1\rangle\left|\frac{1}{2},\frac{1}{2}\right\rangle\left|J,-\frac{1}{2},M\right\rangle\right), \qquad (12)\end{aligned}$$

$$\begin{aligned}|\Pi_{3/2}\rangle &= \left|0,0,1,(1),\frac{1}{2},\frac{1}{2},J,\frac{3}{2},M,p\right\rangle \\ &= \frac{1}{\sqrt{2}}|0,0\rangle\left(|1\rangle\left|\frac{1}{2},\frac{1}{2}\right\rangle\left|J,\frac{3}{2},M\right\rangle\right. \\ &\quad \left. + \chi_p|-1\rangle\left|\frac{1}{2},-\frac{1}{2}\right\rangle\left|J,-\frac{3}{2},M\right\rangle\right), \qquad (13)\end{aligned}$$

$$\begin{aligned}|\Sigma^+_{1/2}\rangle &= \left|1,1,1,(0),\frac{1}{2},\frac{1}{2},J,\frac{1}{2},M,p\right\rangle \\ &= \frac{1}{2}(|1,1\rangle|-1\rangle + |1,-1\rangle|1\rangle)\left(\left|\frac{1}{2},\frac{1}{2}\right\rangle\left|J,\frac{1}{2},M\right\rangle\right. \\ &\quad \left. + \chi_p\left|\frac{1}{2},-\frac{1}{2}\right\rangle\left|J,-\frac{1}{2},M\right\rangle\right), \qquad (14)\end{aligned}$$

where the parity-dependent phase is $\chi_p = (-1)^{J-S}p$.

We can write rotational energy by adding vibrational angular momentum $\boldsymbol{G}$ to the usual expression:

$$\begin{aligned}H_{\rm rot} &= B(\boldsymbol{J} - \boldsymbol{G} - \boldsymbol{L} - \boldsymbol{S})^2 = B[J(J+1) - \Omega^2] \\ &\quad - 2B\sum_{q=\pm1}[J_qG_q + J_qL_q + J_qS_q \\ &\quad + G_qL_{-q} + G_qS_{-q} + L_qS_{-q}] \\ &\quad - B\sum_{q=\pm1}[G_qG_{-q} + L_qL_{-q} + S_qS_{-q}]. \qquad (15)\end{aligned}$$

Here we use the recipe from Ref. [36] that in the molecular frame all scalar products involving total angular momentum $\boldsymbol{J}$ are written as $J_q X_q$ rather than $(-1)^q J_q X_{-q}$. The last line of Eq. (15) can be skipped because it gives a constant independent of J, Ω, and p. The terms in the third line of Eq. (15) linear in L_q turn to zero in the subspace $\Lambda = \pm 1$. We are left with the following operator for the rotational energy:

$$H_{\rm rot} = B[J(J+1) - \Omega^2] - D[J(J+1) - \Omega^2]^2 - 2B \sum_{q=\pm 1} [J_q G_q + J_q S_q + G_q S_{-q}], \quad (16)$$

where we added a standard centrifugal correction to the main diagonal term.

It is straightforward to calculate MEs of this operator on the states (12)–(14). The term $J_q S_q$ does not change quantum number l and cannot mix Σ and Π states. The nonzero matrix elements are

$$\langle \Pi_{3/2}| - 2B J_q S_q |\Pi_{1/2}\rangle = -B\sqrt{\left(J - \tfrac{1}{2}\right)\left(J + \tfrac{3}{2}\right)}, \quad (17)$$

$$\langle \Sigma^+_{1/2}| - 2B J_q S_q |\Sigma^+_{1/2}\rangle = -B\chi_p\left(J + \tfrac{1}{2}\right). \quad (18)$$

The operator $J_q G_q$ changes quantum number l by one and mixes Σ and Π states:

$$\langle \Sigma^+_{1/2}| - 2B J_q G_q |\Pi_{1/2}\rangle = -\beta\chi_p\left(J + \tfrac{1}{2}\right), \quad (19)$$

$$\langle \Sigma^+_{1/2}| - 2B J_q G_q |\Pi_{3/2}\rangle = \beta\sqrt{\left(J - \tfrac{1}{2}\right)\left(J + \tfrac{3}{2}\right)}, \quad (20)$$

where β is defined as

$$\beta = B\langle l = 1|G_1|l = 0\rangle. \quad (21)$$

This ME cannot be calculated within this formalism and is included as an independent parameter of the effective Hamiltonian (see also Sec. IV). Finally, the term $G_q S_{-q}$ mixes Σ and Π states, but cannot change the quantum number Ω:

$$\langle \Sigma^+_{1/2}| - 2B G_q S_{-q} |\Pi_{1/2}\rangle = -\beta. \quad (22)$$

In addition to the rotational energy the effective Hamiltonian must include the spin-orbit interaction (3), the energy splitting $\Delta E_{\Sigma\Pi}$ between Σ and Π states, and the spin-rotation interaction. Following Ref. [36] we write the latter as

$$\gamma(\boldsymbol{N}\boldsymbol{S}) = \gamma(\boldsymbol{J} - \boldsymbol{S})\boldsymbol{S} = \gamma\left(\Omega\Sigma + \sum_{q=\pm 1} J_q S_q - S(S+1)\right). \quad (23)$$

The nontrivial part of this interaction is now reduced to the MEs (17) and (18).

Equations (19)–(22) show that the Coriolis terms involving vibrational angular momentum $\boldsymbol{G}$ lead to the K doubling via the interaction between Π and Σ states. In contrast with the terms involving electronic angular momentum $\boldsymbol{L}$, here we do not need mixing with excited electronic states. Still, because of the relative smallness of the parameter β in Eq. (21), these latter terms cannot be neglected. They have exactly the same form as for diatomic molecules and are defined in Ref. [36].

Transition amplitudes between spin-rotational states of the l-C_3H molecule are expressed through MEs of the dipole moment operator $\boldsymbol{D}$ on the basic states (12)–(14). Generally, speaking there are both diagonal and nondiagonal MEs in vibrational quantum numbers v, l. Let us estimate them using atomic units ($\hbar = m_e = |e| = 1$).

In the molecular frame the diagonal ME is reduced to the dipole moment of the molecule along the molecular axis $\langle v,l|D_\zeta|v,l\rangle \approx D$. If we assume that the charge of the hydrogen atom in the molecule is q, then $D \sim 2qR_0 \sim 4q$, where R_0 is the bond length. Comparing this estimate with the calculated value $D = 1.40$ [37] we get $q = 0.35$. Now we can estimate the nondiagonal ME: $\langle 0,0|D_1|1,-1\rangle \sim q\bar{\xi} \sim q/\sqrt{M\omega_v} \sim qM^{-1/4} \sim 0.1q \sim 0.04$, where $\bar{\xi}$ is the amplitude of the vibration and $M \sim 10^4$ is the reduced mass for this vibration mode. We conclude that nondiagonal MEs are much smaller than diagonal, so we will neglect them.

In this approximation we get the following expressions for the reduced MEs on the basis states (12)–(14):

$$\langle X_\Omega, J', p'||D||Y_\Omega, J, p\rangle = \delta_{X,Y}(-1)^{J'-\Omega}\sqrt{(2J'+1)(2J+1)} \times \begin{pmatrix} J' & 1 & J \\ -\Omega & 0 & \Omega \end{pmatrix} \frac{1 - p'p}{2} D, \quad (24)$$

where X and Y denote either a Π state or a Σ state. Below we use these expressions and the theoretical value $D = 1.40$ a.u. [37] to estimate reduced MEs for the microwave transitions in l-C_3H. The Einstein coefficients A for these transitions can be found as [38]

$$A_{i\to j} = \frac{4\omega_{ij}^3}{3\hbar c} \frac{|\langle i||D||j\rangle|^2 a_0^2}{2J_i + 1}, \quad (25)$$

where the reduced ME is in a.u. and a_0 is the Bohr radius.

IV. SCALING OF PARAMETERS OF EFFECTIVE HAMILTONIAN WITH α AND μ

The effective Hamiltonian described in Sec. III is essentially equivalent to the one used in Ref. [14]. We included centrifugal corrections to most of the terms using the same definitions as in Ref. [14]. For the hyperfine structure we used usual parameters a, b, c, and d. Note that in Ref. [14] the constant $b_F = b + c/3$ was used instead of b.

In this section we discuss how the parameters of the effective Hamiltonian depend on the constants α and μ (see Table III). The scaling of the two largest parameters $\Delta E_{\Sigma\Pi} \sim \mu^{1/2}$ and $A_{\rm eff} \sim \alpha^2$ has been already discussed in Sec. II. The rotational constants B_Σ and B_Π depend linearly on μ. The spin-rotational interaction (23) appears from the second-order cross term in Coriolis and spin-orbit interactions; therefore $\gamma \sim \alpha^2\mu$. For Π states there are two additional terms of the spin-rotational interaction with parameters p and q. The first has the same scaling, as γ, i.e., $p \sim \alpha^2\mu$. The second term is quadratic in the Coriolis interaction, so $q \sim \mu^2$. These scalings are obvious from the expressions on pp. 362 and 531 of Ref. [36].

TABLE III. Parameters of effective rotational Hamiltonian and their scaling with α and μ.

Param.	This work	Ref. [14]	Units	Scaling
$\Delta E_{\Sigma\Pi}$	609.9811	609.9742	GHz	$\alpha^0\mu^{1/2}$
B_Σ	11.2124327	11.2126703	GHz	$\alpha^0\mu^1$
D_Σ	4.548	4.867	kHz	$\alpha^0\mu^2$
γ_Σ	−35.800	−35.525	MHz	$\alpha^2\mu^1$
$\gamma_{\Sigma,D}$	18.04	0.549	kHz	$\alpha^2\mu^2$
b_Σ	−6.3	−6.29	MHz	$\alpha^2\mu^1$
c_Σ	31.8	27.17	MHz	$\alpha^2\mu^1$
$A_{\rm eff}$	432.7762	432.7898	GHz	$\alpha^2\mu^0$
B_Π	11.1892055	11.1891033	GHz	$\alpha^0\mu^1$
D_Π	5.356	5.2340	kHz	$\alpha^0\mu^2$
γ_Π	−48.652	−48.075	MHz	$\alpha^2\mu^1$
$\gamma_{\Pi,D}$	21.670	0.000	kHz	$\alpha^2\mu^2$
p	−6.9021	−7.0681	MHz	$\alpha^2\mu^1$
p_D	−1.595	0.504	kHz	$\alpha^2\mu^2$
q	−12.8556	−12.9922	MHz	$\alpha^0\mu^2$
q_D	−0.443	−0.1432	kHz	$\alpha^2\mu^3$
β	1.2586	1.2342	GHz	$\alpha^0\mu^{5/4}$
β_D	−28.3	−19.2	kHz	$\alpha^0\mu^{9/4}$
a_Π	12.43	12.32	MHz	$\alpha^2\mu^1$
b_Π	−22.57	−23.04	MHz	$\alpha^2\mu^1$
c_Π	27.56	28.07	MHz	$\alpha^2\mu^1$
d_Π	16.21	16.26	MHz	$\alpha^2\mu^1$

Let us now discuss the parameter β defined by Eq. (21). It is proportional to the nondiagonal ME $\langle 1|G_1|0\rangle$. According to Eq. (13) in Ref. [32], the perpendicular component G_1 simultaneously depends on the vibrational coordinates of the bending (v_b) and stretching (v_s) modes. In the harmonic approximation it has nonzero MEs only between different stretching vibrational states, i.e.,

$$\langle v_b = 1, v_s = 1|G_1|v_b = 0, v_s = 0\rangle \neq 0.$$

The ME in Ref. (21) is diagonal in stretching quantum number v_s. It is nonzero due to the anharmonic corrections which mix vibrational modes. Such corrections appear in the first order of the adiabatic perturbation theory and are proportional to the adiabatic expansion parameter $\mu^{1/4}$. Thus we can expect that $\beta \sim 0.1B$. This estimate agrees well with the numerical value obtained in Sec. V. We conclude that $\beta \sim \mu^{1/4}B \sim \mu^{5/4}$.

Our effective Hamiltonian includes centrifugal corrections (D, γ_D, β_D, etc.) to the most important terms. We assume that such corrections have the same α dependence as the respective main term and an extra power in their μ dependence. The magnetic hyperfine constants scale as the product of the nuclear and electronic magnetic moments, i.e., as $\alpha^2\mu$.

All scalings discussed above are approximate. There are relativistic corrections to all parameters, which modify their α dependence. These corrections are of the order of $(\alpha Z)^2 \sim 0.2\%$. The μ dependence of parameters is changed by nonadiabatic corrections. To illustrate this point let us consider the rotational constants B. To a first approximation the small difference between B_Σ and B_Π can be related to the vibrational corrections to the adiabatic value of the rotational constant B_0.

We can use the data from Table I and Table III to estimate the vibrational correction to the rotational constant:

$$B_v = B_0 - \alpha(v+1), \tag{26}$$

$$B_0 = \frac{(v_\Sigma+1)B_\Pi - (v_\Pi+1)B_\Sigma}{v_\Sigma - v_\Pi} = 11\,137.1\,\text{MHz}, \tag{27}$$

$$\alpha = \frac{B_\Pi - B_\Sigma}{v_\Sigma - v_\Pi} = -22.8\,\text{MHz}. \tag{28}$$

If we assume that B_0 scales as μ and α scales as $\mu^{3/2}$ [5], we get the following scalings of the rotational constants from Table III:

$$B_\Sigma \sim \mu^{1.010}, \quad B_\Pi \sim \mu^{1.007}. \tag{29}$$

Note that we neglected other vibrational degrees of freedom, so actual corrections can be somewhat bigger. We conclude that we know the scalings of the main parameters from Table III roughly to one percent accuracy. Further improvement of this accuracy requires extensive *ab initio* calculations.

V. NUMERICAL RESULTS FOR ROTATING MOLECULE

Our effective Hamiltonian has 22 parameters listed in Table III including 6 parameters for the hyperfine structure. The 16 nonhyperfine parameters were fit using the simplex method to the 44 experimentally observed transitions from Ref. [14] and to 12 experimental frequencies listed in the NIST database [39]. We added 8 theoretically predicted transitions for lower rotational quantum numbers from the same database to be sure we adequately reproduce this part of the spectrum.

In our fit the rms deviation for 64 fitted transitions is 0.23 MHz with maximum deviation 0.52 MHz. This accuracy is lower than the typical accuracy of the similar fits in the literature but is absolutely sufficient for our purposes. Our main goal here is to calculate sensitivity coefficients for different transitions to the variation of the fundamental constants. Although the sufficiently complex effective Hamiltonians allow for very accurate predictions of the transition frequencies, the accuracy they can provide for the sensitivity coefficients is limited by the uncertainty in the dependence of the parameters used on the fundamental constants (see Sec. IV and Ref. [5]).

To fit the hyperfine structure parameters we used 30 lines from the Ref. [19] and 12 K-doublet transitions from [40]. The hyperfine structure is mostly too small to change the values of the sensitivity coefficients. This in not true only for several K-doublet transitions with frequencies $\lesssim$100 MHz, comparable to the hyperfine splittings. We used the scalings from Table III to calculate the shifts of the spin-rotational levels due to the change of the constants α and μ by $\pm 0.1\%$. After that we found dimensionless sensitivities Q_α and Q_μ for the transitions described by the effective Hamiltonian.

There are three manifolds of levels, which belong to the vibronic states $\Pi_{1/2}$, $\Pi_{3/2}$, and $\Sigma^+_{1/2}$ (see Fig. 1). According to Ref. [24] the strongest transitions take place between levels of the same manifold. The higher-frequency transitions correspond to the change of the rotational quantum number $J \to J+1$ (see Table IV). Such transitions usually have $Q_\alpha \approx 0$, $Q_\mu \approx 1$ [41]. We see that this is also true for l-C_3H.

For the $\Pi_{1/2}$ and $\Pi_{3/2}$ manifolds there is weak monotonic dependence of the sensitivities on J. This dependence is

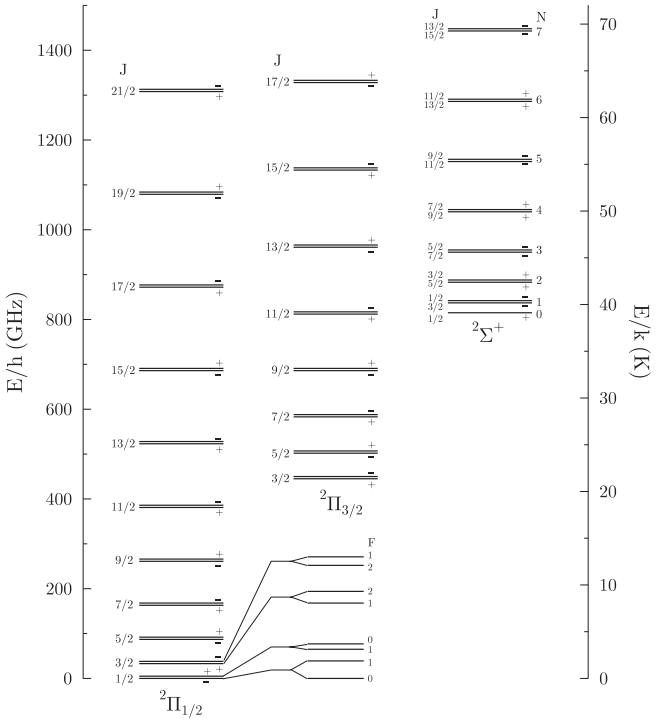

FIG. 1. Spin-rotational levels of the three lowest vibronic states of the molecule l-C_3H. K doubling is shown schematically. The levels are labeled by the quantum numbers J and p. The hyperfine structure for the two lowest K doublets is shown in the inset. Due to a strong Renner-Teller effect the component $^2\Sigma^+$ of the excited bending state ν_4(CCH bending) is shifted towards lower energies, $\sim$29 cm^{-1} above the zero-level of the ground state $^2\Pi_{1/2}$.

caused by the Coriolis interaction between these manifolds. For the upper part of the $\Pi_{3/2}$ spectrum we see some irregularities in sensitivities. They are caused by the resonant interactions with the nearby levels of the $\Sigma_{1/2}$ manifold, where similar irregularities are observed for $N \geqslant 22$. All these irregularities are weak because interaction energy is much smaller than respective transition frequencies.

For the Π states there are also lower-frequency transitions between the levels of different parity with the same J (K doublets). For diatomic radicals such transitions are known to be very sensitive to the variation of both constants [8–10]. Electron spin gradually decouples from the molecular axis with growing rotational energy. As a result, the Ω doubling for low-J values transforms to Λ doubling for higher Js. In our case the electronic quantum number Λ is substituted by the vibronic quantum number K; otherwise the effects are rather similar (see Tables V and VI). Decoupling of the electron spin happens around $J = \frac{13}{2}$ and causes the anomaly in sensitivities for the $\Pi_{1/2}$ doublets around $J = \frac{13}{2}$, where the frequency drops below 50 MHz. For the l-C_3H molecule we can expect additional anomalies in sensitivities due to the proximity and strong interaction of Π and Σ states [35]. One such anomaly is caused by the resonance between the levels $\Pi_{3/2}$ and $\Sigma^+_{1/2}$ with $J \approx \frac{49}{2}$. The transition frequency is higher here, about 1 GHz, but this is much smaller than for the neighboring rotational states.

The hyperfine structure is much larger for the K doublets of the $\Pi_{1/2}$ state. For this reason we do not neglect the hyperfine structure in Table V. For high-J values the transitions with $\Delta F \neq 0$ are strongly suppressed, so we list only transitions with $\Delta F = 0$. In Table VI the hyperfine splitting is neglected for all but the first few transitions. For transitions with $J \geqslant \frac{7}{2}$ the sensitivity coefficients for the hyperfine components of the transition are practically the same.

Because of the mixings (17)–(22) of the basic states there are also weaker transitions between the $\Pi_{1/2}$, $\Pi_{3/2}$, and $\Sigma^+_{1/2}$ manifolds. Examples of such transitions are listed in Tables VII and VIII. Sensitivities of these transitions depend on the quantum numbers in a less regular manner, than sensitivities within each manifold.

TABLE IV. Frequencies (MHz), Q factors, and reduced MEs (a.u.) of some rotational transitions for $\Pi_{1/2}$, $\Pi_{3/2}$, and $\Sigma^+_{1/2}$ states.

$J \to J+1$ transitions for $\Pi_{1/2}$ state					
$J'\ p'$	$J\ p$	ω	Q_α	Q_μ	$\|\|D\|\|^2$
$\frac{3}{2}+$	$\frac{1}{2}-$	32627.84	0.06 (0)	0.97 (1)	1.86
$\frac{3}{2}-$	$\frac{1}{2}+$	32662.10	0.06 (0)	0.97 (1)	1.86
$\frac{5}{2}-$	$\frac{3}{2}+$	54405.75	0.06 (0)	0.97 (1)	3.33
$\frac{5}{2}+$	$\frac{3}{2}-$	54428.34	0.06 (0)	0.97 (1)	3.33
$\frac{7}{2}+$	$\frac{5}{2}-$	76199.10[a]	0.06 (0)	0.97 (1)	4.72
$\frac{7}{2}-$	$\frac{5}{2}+$	76204.62[a]	0.06 (0)	0.97 (1)	4.72
$\frac{35}{2}-$	$\frac{33}{2}+$	383435.12[b]	0.02 (0)	0.99 (1)	18.51
$\frac{35}{2}+$	$\frac{33}{2}-$	383942.45[b]	0.02 (0)	0.99 (1)	18.72
$\frac{47}{2}-$	$\frac{45}{2}+$	516312.64[b]	0.01 (0)	0.99 (1)	22.39
$\frac{49}{2}-$	$\frac{47}{2}+$	539280.62[b]	0.01 (0)	0.99 (1)	23.43
$J \to J+1$ transitions for $\Pi_{3/2}$ state					
$J'\ p'$	$J\ p$	ω	Q_α	Q_μ	$\|\|D\|\|^2$
$\frac{5}{2}-$	$\frac{3}{2}+$	57437.17	−0.05 (1)	1.03 (1)	2.22
$\frac{5}{2}+$	$\frac{3}{2}-$	57453.77	−0.06 (0)	1.03 (1)	2.22
$\frac{7}{2}+$	$\frac{5}{2}-$	80388.41	−0.05 (0)	1.03 (1)	3.93
$\frac{7}{2}-$	$\frac{5}{2}+$	80421.07	−0.05 (0)	1.03 (1)	3.93
$\frac{47}{2}-$	$\frac{45}{2}+$	532658.83[b]	−0.06 (0)	0.98 (1)	17.54
$\frac{49}{2}-$	$\frac{47}{2}+$	556392.87	−0.01 (0)	1.00 (1)	23.16
$\frac{49}{2}+$	$\frac{47}{2}-$	552385.85[b]	−0.12 (0)	0.94 (1)	13.61
$\frac{51}{2}-$	$\frac{49}{2}+$	599557.31	0.09 (1)	1.00 (1)	14.29
$\frac{51}{2}+$	$\frac{49}{2}-$	578834.56	−0.01 (0)	1.00 (1)	23.77
$\frac{53}{2}-$	$\frac{51}{2}+$	601263.86	−0.01 (0)	1.00 (1)	24.38
$N \to N+1$ transitions for $\Sigma^+_{1/2}$ state					
$N'\ J'\ p'$	$N\ J\ p$	ω	Q_α	Q_μ	$\|\|D\|\|^2$
$1\ \frac{1}{2}-$	$0\ \frac{1}{2}+$	22468.22	0.00 (0)	1.00 (1)	0.93
$1\ \frac{3}{2}-$	$0\ \frac{1}{2}+$	22420.66	0.00 (0)	1.00 (1)	1.87
$2\ \frac{3}{2}+$	$1\ \frac{1}{2}-$	44888.43	0.00 (0)	1.00 (1)	1.87
$2\ \frac{5}{2}+$	$1\ \frac{3}{2}-$	44857.31	0.00 (0)	1.00 (1)	3.36
$23\ \frac{47}{2}-$	$22\ \frac{45}{2}+$	517808.87[b]	0.05 (0)	1.02 (1)	26.02
$24\ \frac{47}{2}+$	$23\ \frac{45}{2}-$	538178.20	0.00 (0)	1.00 (1)	32.57
$24\ \frac{49}{2}+$	$23\ \frac{47}{2}-$	542975.34	0.11 (0)	1.07 (2)	19.58
$25\ \frac{49}{2}-$	$24\ \frac{47}{2}+$	560575.62	0.00 (0)	1.00 (1)	33.93
$25\ \frac{51}{2}-$	$24\ \frac{49}{2}+$	540680.86	−0.11 (1)	1.01 (2)	18.11
$26\ \frac{53}{2}+$	$25\ \frac{51}{2}-$	586696.44	−0.07 (0)	0.94 (1)	23.27

[a]Transitions detected at the redshift $z = 0.89$ in Ref. [30].
[b]Transitions observed in Ref. [14].

TABLE V. Frequencies (MHz), Q factors and reduced MEs (a.u.) for K-doubling transitions in $\Pi_{1/2}$ state.

$JF'p', Fp$	ω	Q_α	Q_μ	$\|D\|^2$
$\frac{1}{2}\,1+,\,0-$	52.37	0.66 (2)	1.7 (2)	0.333
$\frac{1}{2}\,0+,\,1-$	39.12	0.20 (2)	1.9 (2)	0.333
$\frac{1}{2}\,1+,\,1-$	34.93	−0.02 (2)	2.0 (2)	0.667
$\frac{3}{2}\,1-,\,1+$	85.55	0.65 (2)	1.7 (1)	0.166
$\frac{3}{2}\,2-,\,1+$	78.60	0.55 (2)	1.7 (1)	0.033
$\frac{3}{2}\,1-,\,2+$	75.23	0.43 (2)	1.8 (1)	0.033
$\frac{3}{2}\,2-,\,2+$	68.29	0.30 (2)	1.8 (1)	0.299
$\frac{5}{2}\,2+,\,2-$	107.19	0.95 (2)	1.5 (1)	0.132
$\frac{5}{2}\,3+,\,2-$	98.97	0.89 (2)	1.5 (1)	0.009
$\frac{5}{2}\,2+,\,3-$	98.83	0.82 (2)	1.6 (1)	0.009
$\frac{5}{2}\,3+,\,3-$	90.61	0.75 (2)	1.6 (1)	0.188
$\frac{7}{2}\,3-,\,3+$	112.38	1.63 (2)	1.2 (1)	0.105
$\frac{7}{2}\,4-,\,4+$	96.07	1.56 (2)	1.2 (1)	0.136
$\frac{9}{2}\,4+,\,4-$	95.75	3.22 (4)	0.36 (7)	0.086
$\frac{9}{2}\,5+,\,5-$	79.63	3.45 (4)	0.23 (7)	0.105
$\frac{11}{2}\,5-,\,5+$	52.81	9.1 (6)	−2.6 (3)	0.072
$\frac{11}{2}\,6-,\,6+$	36.85	12.1 (6)	−4.1 (3)	0.085
$\frac{13}{2}\,6-,\,6+$	20.25	−34. (2)	19. (2)	0.062
$\frac{13}{2}\,7-,\,7+$	36.06	−18. (2)	11. (2)	0.071
$\frac{15}{2}\,7+,\,7-$	126.59	−7.6 (2)	5.8 (4)	0.054
$\frac{15}{2}\,8+,\,8-$	142.24	−6.5 (2)	5.3 (4)	0.061
$\frac{17}{2}\,8-,\,8+$	268.76	−4.7 (1)	4.4 (3)	0.047
$\frac{17}{2}\,9-,\,9+$	284.25	−4.3 (1)	4.2 (3)	0.053
$\frac{19}{2}\,9+,\,9-$	448.75	−3.59 (7)	3.8 (3)	0.042
$\frac{19}{2}\,10+,\,10-$	464.07	−3.39 (7)	3.7 (3)	0.046
$\frac{21}{2}\,10-,\,10+$	668.02	−2.97 (6)	3.5 (3)	0.038
$\frac{21}{2}\,11-,\,11+$	683.18	−2.85 (6)	3.4 (3)	0.041

TABLE VI. Frequencies (MHz), Q factors, and reduced MEs (a.u.) for K-doubling transitions in $\Pi_{3/2}$ state.

$JF'p', Fp$	ω	Q_α	Q_μ	$\|D\|^2$
$\frac{3}{2}\,1-,1+$	5.61	−2.63 (8)	3.2 (2)	1.493
$\frac{3}{2}\,2-,1+$	18.50	0.49 (8)	1.7 (2)	0.299
$\frac{3}{2}\,1-,2+$	−7.30	5.28 (8)	−0.6 (2)	0.299
$\frac{3}{2}\,2-,2+$	5.58	−2.63 (8)	3.2 (2)	2.688
$\frac{5}{2}\,2+,2-$	22.24	−2.60 (8)	3.2 (2)	1.186
$\frac{5}{2}\,3+,2-$	31.50	−1.35 (8)	2.6 (2)	0.085
$\frac{5}{2}\,2+,3-$	12.88	−5.67 (8)	4.6 (2)	0.085
$\frac{5}{2}\,3+,3-$	22.15	−2.60 (8)	3.2 (2)	1.694
$\frac{7}{2}\,3-,3+$	54.92	−2.57 (8)	3.2 (2)	0.943
$\frac{7}{2}\,4-,4+$	54.76	−2.57 (8)	3.2 (2)	1.223
$\frac{9}{2}+-$	108.13	−2.50 (8)	3.1 (2)	1.230
$\frac{11}{2}-+$	185.99	−2.46 (8)	3.1 (2)	1.007
$\frac{13}{2}+-$	291.71	−2.41 (9)	3.0 (2)	0.847
$\frac{15}{2}-+$	427.87	−2.35 (8)	3.0 (2)	0.727
$\frac{17}{2}+-$	596.34	−2.30 (8)	2.9 (2)	0.633
$\frac{19}{2}-+$	798.28	−2.25 (8)	2.9 (2)	0.558
$\frac{21}{2}+-$	1034.16	−2.21 (9)	2.9 (2)	0.497
$\frac{23}{2}-+$	1303.72	−2.17 (9)	2.8 (2)	0.446
$\frac{25}{2}+-$	1605.97	−2.15 (9)	2.8 (1)	0.403
$\frac{27}{2}-+$	1939.08	−2.13 (9)	2.8 (1)	0.366
$\frac{29}{2}+-$	2300.16	−2.13 (9)	2.7 (1)	0.334
$\frac{31}{2}-+$	2684.91	−2.2 (1)	2.7 (1)	0.306
$\frac{33}{2}+-$	3086.93	−2.2 (1)	2.7 (1)	0.282
$\frac{35}{2}-+$	3496.51	−2.4 (1)	2.6 (1)	0.261
$\frac{37}{2}+-$	3898.24	−2.5 (1)	2.60 (9)	0.242
$\frac{39}{2}-+$	4266.17	−2.9 (1)	2.53 (8)	0.224
$\frac{41}{2}+-$	4553.04	−3.5 (1)	2.42 (5)	0.208
$\frac{43}{2}-+$	4663.43	−4.6 (2)	2.2 (1)	0.192
$\frac{45}{2}+-$	4377.16	−7.5 (2)	1.4 (3)	0.174
$\frac{47}{2}-+$	3097.96	−19.0 (4)	−2.3 (9)	0.149
$\frac{49}{2}-+$	909.06	132. (2)	53. (8)	0.103
$\frac{51}{2}-+$	19813.69	−3.11 (5)	−1.6 (4)	0.116
$\frac{53}{2}+-$	16952.67	−1.31 (2)	0.0 (4)	0.136
$\frac{55}{2}-+$	16218.56	−0.61 (2)	0.8 (4)	0.138

All transitions in Table VII have frequencies higher than 100 GHz. Because of that the sensitivity coefficients are not very high, but they are dispersed within intervals $0 \lesssim Q_\alpha \lesssim 4$ and $-1 \lesssim Q_\mu \lesssim 1$. Note that in order to study possible variations of fundamental constants we need to compare several transitions with *different* sensitivities. Thus, such a spread in sensitivities can be very useful [41].

In Table VIII there are several low-frequency transitions with very high sensitivities. Among them there are few with sufficiently high transition amplitudes. In particular, there are three rather strong transitions at 27.6 GHz, 25.1 GHz, and 10.5 GHz with sensitivities Q_α from -5 to $+19$ and Q_μ from -3 to $+11$. This is comparable to the sensitivities of the K-doublet transitions from Tables V and VI, but for higher transition frequencies.

Transitions observed in Ref. [14] are marked with asterisk in Tables IV and VIII. All of them have frequencies above 300 GHz and sensitivities which are not very far from the typical rotational sensitivities: $Q_\alpha \approx 0$ and $Q_\mu \approx 1$. The maximum difference in sensitivities $\Delta Q_\alpha \approx 0.7$ and $\Delta Q_\mu \approx 0.4$ corresponds to the transitions at 535.6 and 571.0 GHz from Table VIII. The only two transitions which were detected at high redshifts in Ref. [30] are marked with the dagger in Table IV. These transitions have much lower frequencies, but they are essentially rotational transitions with "normal" sensitivities.

Let us discuss the accuracy of our calculations of the sensitivity coefficients Q_α and Q_μ. As we mentioned above, we know the scalings of the parameters of the effective Hamiltonian with approximately 1% accuracy. So, we did several calculations of the sensitivity coefficients. First, we changed all scalings by 1%. Second, we used scaling of the rotational constants from Eq. (29) keeping all other scalings unchanged. The uncertainty in the scalings of the smaller parameters of the effective Hamiltonian may be higher due to the nonadiabatic corrections. So we did two additional calculations with the scaling of the parameter β changed by $\pm 1/4$, i.e., $\beta \sim \mu$ and $\beta \sim \mu^{3/2}$. Finally, in order to check

TABLE VII. Frequencies (MHz), Q factors, and reduced MEs (a.u.) of some transitions $\Pi_{1/2}\, J\, p \to \Pi_{3/2}\, J'\, p'$.

$J'p'$	Jp	ω	Q_α	Q_μ	$\|D\|^2$
$\frac{15}{2}-$	$\frac{17}{2}+$	262072.96	3.00 (2)	−0.50 (0)	0.41
$\frac{17}{2}-$	$\frac{17}{2}+$	456425.35	1.70 (2)	0.15 (0)	1.20
$\frac{19}{2}-$	$\frac{17}{2}+$	674795.09	1.14 (1)	0.43 (1)	0.87
$\frac{15}{2}+$	$\frac{17}{2}-$	261366.66	3.02 (2)	−0.51 (0)	0.40
$\frac{17}{2}+$	$\frac{17}{2}-$	456743.26	1.70 (2)	0.15 (0)	1.20
$\frac{19}{2}+$	$\frac{17}{2}-$	673718.38	1.14 (1)	0.43 (0)	0.84
$\frac{31}{2}-$	$\frac{33}{2}+$	185259.51	3.45 (2)	−0.71 (1)	2.31
$\frac{33}{2}-$	$\frac{33}{2}+$	558878.68	1.14 (1)	0.43 (1)	5.46
$\frac{35}{2}-$	$\frac{33}{2}+$	961254.71	0.64 (1)	0.68 (1)	3.30
$\frac{31}{2}+$	$\frac{33}{2}-$	179719.83	3.61 (3)	−0.81 (1)	2.24
$\frac{33}{2}+$	$\frac{33}{2}-$	559110.84	1.13 (1)	0.43 (1)	5.49
$\frac{35}{2}+$	$\frac{33}{2}-$	954903.42	0.66 (1)	0.67 (0)	3.20
$\frac{51}{2}-$	$\frac{53}{2}+$	148111.71	2.91 (2)	−1.01 (6)	3.92
$\frac{53}{2}-$	$\frac{53}{2}+$	729561.89	0.67 (1)	0.67 (0)	12.80
$\frac{55}{2}-$	$\frac{53}{2}+$	1369461.89	0.34 (1)	0.82 (1)	6.63
$\frac{51}{2}+$	$\frac{53}{2}-$	118586.34	4.22 (4)	−1.18 (2)	5.69
$\frac{53}{2}+$	$\frac{53}{2}-$	736802.86	0.64 (1)	0.63 (1)	10.93
$\frac{55}{2}+$	$\frac{53}{2}-$	1343531.64	0.36 (1)	0.81 (1)	7.01

how the fitting procedure may affect the results, we did several calculations with slightly different sets of parameters. For example, we made a 13-parameter fit with three centrifugal corrections set to zero: $\gamma_{\Pi,D} = p_D = q_D = 0$. In terms of the obtained frequencies, such a fit is only three times less accurate than our final 16-parametric fit.

In Tables IV–VIII we give the average values of the Q factors for all calculations described above. The errors given in the brackets correspond to the maximum deviations from these average values for individual calculations. In most cases these errors are smaller than or of the order of 10%, even for the large sensitivities. This accuracy is sufficient for the analysis of the experimental and observational data.

VI. CONCLUSION

We have studied the sensitivity of coefficients to the variation of the fundamental constants α and μ for the microwave and submillimeter spectra of the linear polyatomic molecule with strong Renner-Teller interaction. As an example we chose the l-C_3H molecule, which is often observed in the interstellar molecular clouds and which recently has been detected at the redshift $z = 0.89$.

The Renner-Teller interaction depends on the dimensionless ratio $\mathcal{E} = k'/k$ of the force constants in the two perpendicular planes which include the molecular axis. The parameter $\mathcal{E}$ does not depend on the fundamental constants and vibrational intervals scale in the same way as for harmonic oscillator, i.e., $E_v \sim \mu^{1/2}$. However, the Renner-Teller interaction modifies the vibrational spectrum and can lead to the close-lying vibrational states. Such states then strongly interact with each other due to the Coriolis interaction. As a result, the molecules with strong Renner-Teller interaction can have low-frequency mixed rovibronic transitions with strongly enhanced sensitivity coefficients to the variation of α and μ. Note that the term "low frequency" here has a relative meaning. It means that the frequency of the mixed transition is much smaller than the rotational and vibronic energies involved. For the l-C_3H molecule we found several types of transitions with sensitivity coefficients varying over a wide range. This opens new possibilities to study variation of fundamental constants in astrophysics.

TABLE VIII. Frequencies (MHz), Q factors, and reduced MEs (a.u.) of some transitions $\Pi_{3/2}\, J\, p \to \Sigma^+_{1/2}\, N\, J'\, p'$. Negative frequency means that final state lies lower.

$NJ'p'$	Jp	ω	Q_α	Q_μ	$\|D\|^2$
$14\ \frac{29}{2}+$	$\frac{31}{2}-$	−159987.95	2.00 (2)	1.90 (7)	0.10
$16\ \frac{31}{2}+$	$\frac{31}{2}-$	535601.40[a]	−0.60 (1)	0.73 (1)	0.14
$16\ \frac{33}{2}+$	$\frac{31}{2}-$	535512.07	−0.60 (1)	0.73 (1)	0.11
$16\ \frac{33}{2}+$	$\frac{33}{2}-$	161892.90	−1.96 (2)	0.12 (7)	0.21
$15\ \frac{31}{2}-$	$\frac{33}{2}+$	−200166.07	1.55 (2)	1.74 (6)	0.14
$17\ \frac{33}{2}-$	$\frac{33}{2}+$	540214.36[a]	−0.58 (1)	0.73 (2)	0.18
$17\ \frac{35}{2}-$	$\frac{33}{2}+$	540229.47	−0.57 (1)	0.73 (2)	0.15
$17\ \frac{35}{2}-$	$\frac{35}{2}+$	144436.89	−2.13 (2)	−0.01 (8)	0.28
$16\ \frac{33}{2}+$	$\frac{35}{2}-$	−240483.13	1.25 (1)	1.63 (6)	0.19
$18\ \frac{35}{2}+$	$\frac{35}{2}-$	544660.22[a]	−0.55 (1)	0.72 (2)	0.25
$18\ \frac{37}{2}+$	$\frac{35}{2}-$	544828.26	−0.55 (1)	0.72 (2)	0.22
...					
$23\ \frac{47}{2}-$	$\frac{49}{2}+$	−514442.07	0.17 (0)	1.20 (2)	7.13
$25\ \frac{49}{2}-$	$\frac{49}{2}+$	579974.37	−0.24 (1)	0.79 (2)	13.06
$25\ \frac{51}{2}-$	$\frac{49}{2}+$	569214.13[a]	−0.15 (0)	0.90 (1)	6.18
$24\ \frac{47}{2}+$	$\frac{49}{2}-$	18489.70	−13.9 (2)	−8. (1)	0.15
$24\ \frac{49}{2}+$	$\frac{49}{2}-$	27624.21	−5.28 (7)	−3.0 (5)	9.40
$26\ \frac{51}{2}+$	$\frac{49}{2}-$	1162035.24	−0.22 (0)	0.85 (1)	0.14
$25\ \frac{49}{2}-$	$\frac{51}{2}+$	230.75	−1099.(34)	−742. (90)	0.17
$25\ \frac{51}{2}-$	$\frac{51}{2}+$	−10529.49	18.8 (2)	11. (1)	6.95
$27\ \frac{53}{2}-$	$\frac{51}{2}+$	1188561.69	−0.21 (0)	0.85 (1)	0.15
$24\ \frac{49}{2}+$	$\frac{51}{2}-$	−571024.04[a]	0.14 (1)	1.11 (2)	7.26
$26\ \frac{51}{2}+$	$\frac{51}{2}-$	563386.99	−0.34 (1)	0.79 (3)	10.93
$26\ \frac{53}{2}+$	$\frac{51}{2}-$	556353.26	−0.32 (1)	0.84 (2)	5.39
$26\ \frac{51}{2}+$	$\frac{53}{2}-$	−18063.18	13.6 (2)	11. (1)	0.18
$28\ \frac{53}{2}+$	$\frac{53}{2}-$	−25096.91	9.2 (1)	6.7 (8)	3.01
$28\ \frac{55}{2}+$	$\frac{53}{2}-$	1215046.58	−0.20 (0)a	0.86 (2)	0.17

[a]Transitions observed in Ref. [14].

ACKNOWLEDGMENTS

I am grateful to Sergei Levshakov for bringing the l-C_3H molecule to my attention and for the constant interest in this work. I also want to thank Ed Hinds, Vadim Ilyushin, and Wim Ubachs for valuable discussions. This work is partly supported by the Russian Foundation for Basic Research Grants No. 11-02-00943 and No. 11-02-12284-ofi-m and by The Royal Society.

[1] M. G. Kozlov, S. G. Porsev, and D. Reimers, Phys. Rev. A **83**, 052123 (2011).
[2] M. G. Kozlov, Phys. Rev. A **84**, 042120 (2011).
[3] P. Jansen, L.-H. Xu, I. Kleiner, W. Ubachs, and H. L. Bethlem, Phys. Rev. Lett. **106**, 100801 (2011).
[4] P. Jansen, I. Kleiner, L.-H. Xu, W. Ubachs, and H. L. Bethlem, Phys. Rev. A **84**, 062505 (2011).
[5] S. A. Levshakov, M. G. Kozlov, and D. Reimers, Astrophys. J. **738**, 26 (2011).
[6] V. V. Ilyushin, P. Jansen, M. G. Kozlov, S. A. Levshakov, I. Kleiner, W. Ubachs, and H. L. Bethlem, Phys. Rev. A **85**, 032505 (2012).
[7] S. P. Ellingsen, M. A. Voronkov, S. L. Breen, and J. E. J. Lovell, Astrophys. J. **747**, L7 (2012).
[8] J. N. Chengalur and N. Kanekar, Phys. Rev. Lett. **91**, 241302 (2003).
[9] J. Darling, Phys. Rev. Lett. **91**, 011301 (2003).
[10] M. G. Kozlov, Phys. Rev. A **80**, 022118 (2009).
[11] N. Kanekar, G. I. Langstone, J. T. Stocke, L. C. Carilli, and K. L. Menten, Astrophys. J. **746**, L16 (2012).
[12] C. Chin, V. V. Flambaum, and M. G. Kozlov, New J. Phys. **11**, 055048 (2009).
[13] H. L. Bethlem and W. Ubachs, Faraday Discuss. **142**, 25 (2009).
[14] M. Caris, T. F. Giesen, C. Duan, H. S. P. Müller, S. Schlemmer, and K. M. T. Yamada, J. Mol. Spectrosc. **253**, 99 (2009).
[15] W. M. Irvine, P. Friberg, Å. Hjalmarson, L. E. B. Johansson, P. Thaddeus, R. D. Brown, and P. D. Godfrey, Bull. AAS **16**, 877 (1984).
[16] L. E. B. Johansson, C. Andersson, J. Ellder, P. Friberg, A. Hjalmarson, B. Hoglund, W. M. Irvine, H. Olofsson, and G. Rydbeck, Astron. Astrophys. **130**, 227 (1984).
[17] P. Thaddeus, C. A. Gottlieb, A. Hjalmarson, L. E. B. Johansson, W. M. Irvine, P. Friberg, and R. A. Linke, Astrophys. J. **294**, L49 (1985).
[18] S. Yamamoto, S. Saito, M. Ohishi, H. Suzuki, S.-I. Ishikawa, N. Kaifu, and A. Murakami, Astron. J. **322**, L55 (1987).
[19] S. Yamamoto, S. Saito, H. Suzuki, S. Deguchi, N. Kaifu, and S. Ishikawa, Astrophys. J. **348**, 363 (1990).
[20] J. G. Mangum and A. Wootten, Astron. Astrophys. **239**, 319 (1990).
[21] L.-A. Nyman, H. Olofsson, L. E. B. Johansson, R. S. Booth, U. Carlstrom, and R. Wolstencroft, Astron. Astrophys. **269**, 377 (1993).
[22] M. Guelin, R. Lucas, and J. Cernicharo, Astron. Astrophys. **280**, L19 (1993).
[23] B. E. Turner, E. Herbst, and R. Terzieva, Astrophys. J. Suppl., Ser. **126**, 427 (2000).
[24] J. Cernicharo, M. Guélin, and C. Kahane, Astron. Astrophys., Suppl. Ser. **142**, 181 (2000)
[25] D. Fossé, J. Cernicharo, M. Gerin, and P. Cox, Astrophys. J. **552**, 168 (2001).
[26] N. Kaifu, M. Ohishi, K. Kawaguchi, S. Saito, S. Yamamoto, T. Miyaji, K. Miyazawa, S.-I. Ishikawa, C. Noumaru, S. Harasawa *et al.*, Publ. Astron. Soc. Jpn. **56**, 69 (2004).
[27] J. R. Pardo and J. Cernicharo, Astrophys. J. **654**, 978 (2007).
[28] S. V. Kalenskii and L. E. B. Johansson, Astron. Rep. **54**, 1084 (2010).
[29] S. Martín, R. Mauersberger, J. Martín-Pintado, C. Henkel, and S. García-Burillo, in *IAU Symposium*, Vol. 235 (Cambridge University Press, New York, USA, 2005), p. 265P.
[30] S. Muller, A. Beelen, M. Guélin, S. Aalto, J. H. Black, F. Combes, S. Curran, P. Theule, and S. Longmore, Astron. Astrophys. **535**, A103 (2011).
[31] R. Renner, Z. Phys. **92**, 172 (1934).
[32] J. T. Hougen, J. Chem. Phys. **36**, 519 (1962).
[33] M. Kanada, S. Yamamoto, S. Saito, and Y. Osamura, J. Chem. Phys. **104**, 2192 (1996).
[34] M. Perić, M. Mladenović, K. Tomić, and C. M. Marian, J. Chem. Phys. **118**, 4444 (2003).
[35] K. Beloy, M. G. Kozlov, A. Borschevsky, A. W. Hauser, V. V. Flambaum, and P. Schwerdtfeger, Phys. Rev. A **83**, 062514 (2011).
[36] J. Brown and A. Carrington, *Rotational Spectroscopy of Diatomic Molecules* (Cambridge University Press, Cambridge, UK, 2003).
[37] D. E. Woon, Chem. Phys. Lett. **244**, 45 (1995).
[38] I. I. Sobelman, *Atomic Spectra and Radiative Transitions* (Springer-Verlag, Berlin, 1979).
[39] F. J. Lovas, J. Phys. Chem. Ref. Data **33**, 177 (2004).
[40] H. M. Pickett, R. L. Poynter, E. A. Cohen, M. L. Delitsky, J. C. Pearson, and H. S. P. Müller, J. Quantum Spectrosc. Radiat. Transfer **60**, 883 (1998).
[41] A. J. de Nijs, W. Ubachs, and H. L. Bethlem, Phys. Rev. A **86**, 032501 (2012).